This is the accepted manuscript made available via CHORUS. The article has been published as:

Universal function for heavy-ion fusion cross sections

C. L. Jiang, W. F. Henning, B. P. Kay, and K. E. Rehm

Phys. Rev. C **110**, L051604 — Published 20 November 2024

DOI: 10.1103/PhysRevC.110.L051604

, , , ,

Universal function for heavy-ion fusion cross sections

C.L. Jiang,* W.F. Henning, B.P. Kay, and K.E. Rehm
Physics Division, Argonne National Laboratory, Argonne, IL 60439, USA
(Dated: October 3, 2024)

A universal function for heavy-ion fusion cross sections, $Y = \sqrt{\pi} X erfc(-X) + exp(-X^2)$ is proposed. By scaling both the cross section $\sigma(E)$ and the energy E, heavy-ion fusion cross section data are found to follow closely a universal function over the whole energy range. The scaling is developed from either a simple, empirical single-Gaussian barrier distribution model for the representation $d^2(\sigma E)/dE^2$, or the Modified Siwek Wilczynski model. The cross section expressions of these models are analytical, and can be easily used for all heavy-ion fusion excitation functions. Thus a bench marking of heavy-ion fusion excitation functions has been achieved. A general discussion regarding the universal function is given.

PACS numbers:

Fusion reactions are of central interest for the study of heavy-ion collisions. More than a thousand fusion excitation functions have been determined experimentally. Most of these results have been data-based in an online repository [1]. Many fusion reaction studies are performed to investigate reaction dynamics related to the nuclear structures of the involved nuclei, as detailed numerous review articles, e.g. Ref. [2–7].

For applications or bench-marking of the fusion cross sections, it is of interest to see whether it is possible that the excitation functions $\sigma(E)$ of various fusion systems can be transformed into a universal function by scaling both, cross section σ and energy E. Articles devoted to that have been published, e.g. Refs. [8, 9], and most recent one, Ref. [10]. In Ref. [8] a review of that topic was given, with a conclusion that the 'fusion function method' is the most successful procedure to reduce fusion cross sections to date. It was noticed, however, that the fusion function method uses an expression which does not work well for cross sections covering the whole energy range, from well below, to well above the Coulomb barrier, and thus the success of the method is rather limited.

In the present article, an improved universal function is being proposed. It is based on the fact that the fusion cross section formulas from the single-Gaussian barrier distribution model for the representation $d^2(\sigma E)/dE^2$ and the modified Siwek Wilczynski model reproduce very well many heavy ion fusion excitation functions $\sigma(E)$. This includes the low energy region, where fusion hindrance phenomena have been found and many previous theoretical models exhibit overproduction for the fusion excitation functions [5–7, 11–13].

We at first discuss the previous fusion function method and a related one, then describe the suggested new prescription for comparison.

The well known Wong formula was established in 1974 by C. Y. Wong [14]. At that time, during the early stage of heavy-ion experiments, it reproduced the experimental fusion excitation functions very well. Later, measurements of heavy-ion fusion cross sections were extended to lower energies, and thus to a much lower cross section level of nanobarns and below. It was found that the Wong formula only works well at energies higher than the Coulomb barrier, but over-predicts the fusion excitation function at low energies. The fusion cross section expression of the Wong formula, $\sigma_W(E)$ is given by:

$$\sigma_w(E) = \frac{R_w^2}{2E}\hbar\omega \ln[1 + \exp((2\pi/\hbar\omega)(E - V_w))]. \quad (1)$$

Here the parameters, R_w, V_w and $\hbar\omega$ ($W_w = \hbar\omega$ will be used in Table I later) are the radius, the potential barrier, and the curvature of the potential barrier.

A comparison of calculations with the Wong model to the experiment, ^{16}O + ^{208}Pb, whose fusion cross sections are measured over 7 orders of magnitude, is shown in Fig. 1(a). In the figure, symbols are experimental fusion cross sections and the green curve is the prediction from the Wong formula. Obviously, as already mentioned above, at low energies the green curve over-predicts the experimental data by orders of magnitudes.

Canto *et al.,* [9] suggested to use the Wong formula as a basis to obtain a universal function of fusion cross sections. Their main interest was the study of fusion systems from reactions induced by weakly bound nuclei. For those systems, the measured fusion cross sections tend to be at a comparatively large level. They suggested a 'fusion function method' to obtain a universal function from the Wong formula, and take the following scaled expressions for cross section σ and energy E:

$$E_w^{scal} = (2\pi/\hbar\omega)(E - V_w), \quad (2)$$

and

$$\sigma_w^{scal} = \frac{\sigma 2E}{R_w^2\hbar\omega}. \quad (3)$$

The corresponding universal function $Y_w(X)$ is:

$$Y_w = \ln[1 + \exp(X)]. \quad (4)$$

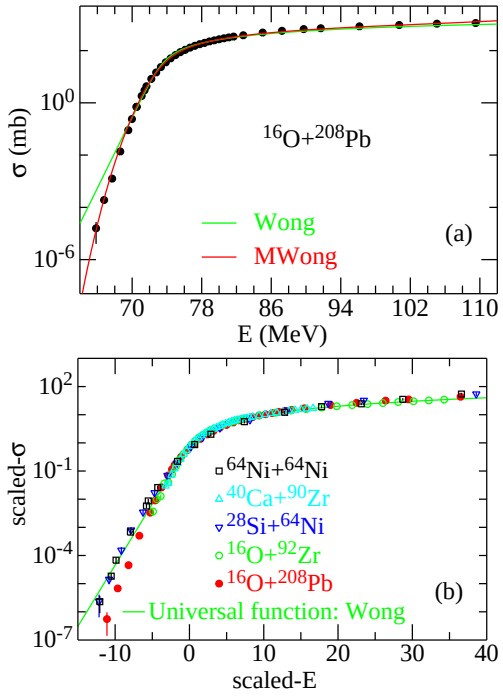


FIG. 1: (a): Spectrum of fusion cross sections of the system ^{16}O + ^{208}Pb [15]. (b): Scaled fusion cross sections based on the Wong formula for the systems ^{16}O + ^{208}Pb [15], ^{16}O + ^{92}Zr [16], ^{28}Si + ^{64}Ni [17], ^{40}Ca + ^{90}Zr [18] and ^{64}Ni + ^{64}Ni [13]. Green and red curves are calculations from the Wong and MWong Model, respectively; parameters are included in Table I.

In the following, Y and X act as the variables on the Y- and the X-axis, respectively, and are plotted together with the experimental data of $scaled-\sigma$ and $scaled-E$, respectively.

In Fig. 1(b), the spectra of the $scaled-\sigma$ vs. $scaled-E$ are compared with the universal function $Y_w(X)$ for five, arbitrarily selected systems (including the system ^{16}O + ^{208}Pb), all measured over wide energy ranges. In the high energy region ($scaled-E>0$) , the data points for these systems are located well on the curve $Y_w(X)$. At low energies, the $Y_w(X)$ over-predicts the experimental data, similar to what is seen in Fig. 1(a). It should be noted that, in Fig. 1(a) and Fig. 1(b), for the system ^{16}O + ^{208}Pb, the green curves are equivalent; they are just the transformations of each other.

Obviously, from the results shown in Fig. 1, the "Fusion function method" is not good enough to serve as a benchmark of the fusion cross sections.

Recently, a modified Wong formula (MWong) [19] (see also Ref. [20]) has been developed, which improves the Wong formula and reproduces the experimental data, even at low energies. The modified Wong formula is based on the Wong formula, but assumes that the parameter $\hbar\omega$ should be energy dependent. It should be noted that, the idea, parameter $\hbar\omega$ should be energy dependent was first discussed in detail in a paper by Rowley and Hagino, [21], and was applied even earlier in their calculations with quantum diffusion approach implicitly by Sargsyam et al., [22], as we know.

In the modified Wong model, there are two parameters $\hbar\omega_f$ and λ to describe the curvature of the potential barrier:

$$\hbar\omega_w -> \hbar\omega_f \exp\big[\lambda\frac{E-V_f}{V_f}\big]. \tag{5}$$

Then the modified Wong formula becomes:

$$\sigma_f(E) = \frac{R_f^2}{2E}\hbar\omega_f \exp\big[\lambda\frac{E-V_f}{V_f}\big] \ln\big[1+ \exp\big((2\pi/\hbar\omega_f \exp\big[\lambda\frac{E-V_f}{V_f}\big])(E-V_f)\big)\big]. \tag{6}$$

In Fig. 1(a), calculations with the Modified Wong formula are included (red curve) and compared with the Wong formula and the experimental fusion cross sections of ^{16}O+^{208}Pb. The parameters of MWong formula are given in Table 1 (there, $W_f = \hbar\omega_f$ will be used). Evidently, the MWong model reproduces the experimental data even at low energies.

From Eq. 6 one notes that the universal function of $Y_f(X)$ is the same as $Y_w(X)$ (MWong):

$$Y_f = Y_w = \ln[1+\exp(X)], \tag{7}$$

but the ways of making $scaled-\sigma$ and $scaled-E$ for the Modified Wong formula are different from the Wong formula:

$$\sigma_f^{scal} = \frac{\sigma 2E}{R_f^2\hbar\omega_f \exp\big[\lambda\frac{E-V_f}{V_f}\big]}, \tag{8}$$

and

$$E_f^{scal} = 2\pi/\big(\hbar\omega_f \exp\big[\lambda\frac{E-V_f}{V_f}\big]\big)(E-V_f), \tag{9}$$

In Fig. 2, for the same five systems shown in Fig. 1(b), the spectra of the $scaled-\sigma$ vs. $scaled-E$ are compared with the universal function $Y_f(X)$. Over the whole energy range, the data points for these systems are now located well on the curve $Y_f(X)$, much improved from the results for the Wong formula at low energies.

However, the modified Wong formula is not a good candidate for the universal function, because, the $scaled-E$ is often not a monotonic function of energy E like in the case of ^{16}O + ^{208}Pb. (See Eq. 9, $scaled-E$ is determined by two factors with a division). This is not good from the point of view of applications. By using this modified Wong model, the proceeding discussion aimed to illustrate a point, that not any formula, even if it can reproduce the cross sections of many systems over the whole energy range, can serve as the basis for establishing a universal function.

TABLE I: Results of the least-squares fits of the Wong formula, Modified Wong formula, and single-Gaussian barrier distribution model, for the fusion systems compared in Figs. 1, 2, 3(a) and 4. Parameters are R_w, V_w and W_w for the Wong model, R_f, V_f, W_f, and λ for the Modified Wong formula, and R_g, V_g and W_g for the single-Gaussian barrier distribution model. For parameters from the MSW model, see Ref. [33] (e.g. for ^{16}O+^{208}Pb: R_0, V_B, W_B, and ΔR are 10.62, 73.79, 1.20 and 1.877). CN is the compound nucleus, N the number of data points, and 'data-range' is the cross section range of the measured values.

system	CN	N	data-range	R_w	V_w	W_w	R_f	V_f	W_f	λ	R_g	V_g	W_g	Ref.
			mb	fm	MeV	MeV	fm	MeV	MeV		fm	MeV	MeV	
^{16}O+^{208}Pb	^{224}Th	38	0.000016-1133	9.69	72.92	4.000	10.39	73.77	6.809	6.409	10.43	73.59	1.575	[15]
^{16}O+^{92}Zr	^{108}Cd	16	0.19-732	9.52	41.40	5.197	9.59	41.55	6.015	2.043	9.56	41.48	1.593	[16]
^{28}Si+^{64}Ni	^{92}Mo	16	0.00003-506	6.71	49.32	2.747	7.97	50.53	5.943	5.240	8.05	50.45	1.398	[17]
^{40}Ca+^{90}Zr	^{130}Nd	40	0.84-407	9.94	96.12	5.368	10.15	96.52	7.371	9.567	10.00	96.18	1.582	[18]
^{64}Ni+^{64}Ni	^{128}Ba	16	0.00002-412	7.83	91.53	2.875	8.99	93.42	8.878	12.16	8.86	92.62	1.452	[13]

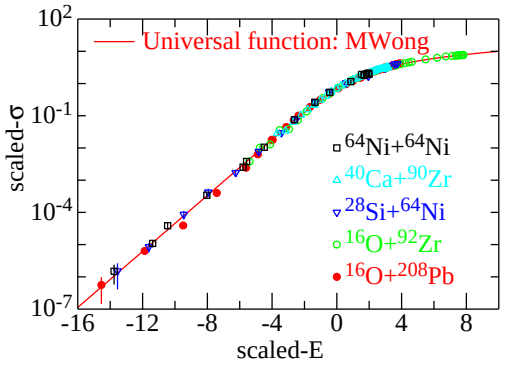


FIG. 2: Scaled cross sections based on the Modified Wong formula for the fusion systems ^{16}O + ^{208}Pb [15], ^{16}O + ^{92}Zr [16], ^{28}Si + ^{64}Ni [17], ^{40}Ca + ^{90}Zr [18] and ^{64}Ni + ^{64}Ni [13]. Parameters are included in Table I. The curve is the calculation for the universal function obtained from the modified Wong formula.

Now we describe the new prescription of a universal function.

The single-Gaussian barrier distribution model is known to reproduce the fusion excitation function rather well, including the energy region below the Coulomb barrier [23–26]. The assumed barrier distribution and the cross section formula are given by:

$$D_g(B) = \frac{1}{\sqrt{2\pi}W_g} exp\Big[-\Big(\frac{B-V_g}{\sqrt{2}W_g}\Big)^2\Big], \qquad (10)$$

and

$$\sigma_g(E) = \frac{\pi R_g^2}{E}\int_{E_0}^{E}\Big(\int_{E_0}^{E'} D_g(E'')dE''\Big)dE'$$
$$= \frac{\sqrt{\pi}R_g^2 W_g}{\sqrt{2}E}\Big[\sqrt{\pi}Zerfc(-Z) + exp(-Z^2)\Big], \qquad (11)$$

where $Z = (E-V_g)/\sqrt{2}W_g$. The parameters, R_g, V_g and W_g are the barrier radius, barrier height and the standard deviation of the distribution.

From Eq. 11 one can demonstrate that, if we assume:

$$E_g^{scal} = (E-V_g)/(\sqrt{2}W_g), \qquad (12)$$

and

$$\sigma_g^{scal} = \frac{\sigma\sqrt{2}E}{\sqrt{\pi}R_g^2 W_g}, \qquad (13)$$

then all the data points will be located very well on the universal function $Y_g(X)$, with the $scaled-\sigma$ and $scaled-E$ as Y-axis and X-axis, respectively:

$$Y_g = \sqrt{\pi}Xerfc(-X) + exp(-X^2). \qquad (14)$$

Fig. 3(a) illustrates that Eq. 14 is a good universal function for the spectra of the $scaled-\sigma$ vs. $scaled-E$ of the same five fusion systems shown in Fig. 1(b). Obviously, all data points overlap and are well reproduced by the curve, which is the result of the universal function $Y_g(X)$ of Eq. 14. It should be noted, that the plots in Fig. 3 and Fig. 4 are logarithmic, spanning many orders of magnitude, and thus with error bars which are often smaller than the data symbols, can work well in the connection with application and bench-marking of heavy-ion fusion. How it relates to the fine structures and underlying physics aspects, is discussed at the end of the article.

It was mentioned above, the selection of these five systems is arbitrary. In fact, as we know all heavy-ion fusion systems (except for some very light systems, e.g. fusion between ^{12}C and ^{16}O nuclei), including those systems which are known with strong fusion enhancements due to couplings from excitation or from transfer reactions, can be well reproduced by the single-Gaussian model and the universal function $Y_g(X)$ (Eq. 14). In order to further illustrate this point, another selection of five fusion systems, are shown in Fig. 3(b). In Ref. [23], parameters for the single-Gaussian model of 29 systems, from ^{16}O + ^{18}O [27] to ^{64}Ni + ^{124}Sn [29, 30] are listed. Here, in Fig. 3(b) we sample three, the lightest, the heaviest, and in-between, of the 29 systems in Ref. [23]. They are: ^{16}O + ^{18}O [27], ^{11}B + ^{197}Au [28], and ^{64}Ni + ^{124}Sn [29, 30].

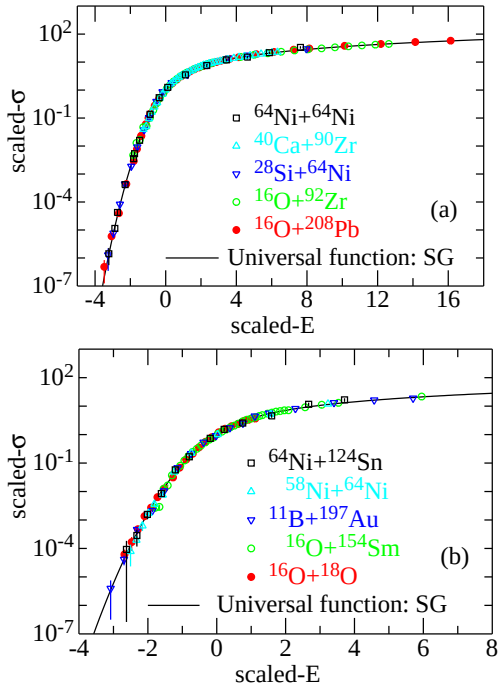


FIG. 3: Spectra of scaled fusion cross sections based on the single-Gaussian Model, (a): for the fusion systems ^{16}O + ^{208}Pb [15], ^{16}O + ^{92}Zr [16], ^{28}Si + ^{64}Ni [17], ^{40}Ca + ^{90}Zr [18] and ^{64}Ni + ^{64}Ni [13]. Parameters are included in Table I; (b): for the fusion systems ^{16}O + ^{18}O [27], ^{16}O + ^{154}Sm [31], ^{11}B + ^{197}Au [28], ^{58}Ni + ^{64}Ni [32], and ^{64}Ni + ^{124}Sn [29, 30]. Parameters are included in Table II. Black curves are the calculations for the universal function of cross sections from the single-Gaussian Model (SG).

In addition, two more fusion systems ^{16}O + ^{154}Sm [31], and ^{58}Ni + ^{64}Ni [32] are included, which are well known in the studies of fusion dynamics that, ^{154}Sm is a deformed nucleus, and cross sections of transfer reaction in ^{58}Ni + ^{64}Ni are rather strong. Obviously, similarly good overlap results are seen in Fig. 3(b) as in 3(a). Parameters R_g, V_g and W_g for these system are listed in Table II, some analyses of them can be found in Ref. [23, 26], respectively.

Recently, Y. Chen *et al.* published a modified Siwek-Wilczynski model (MSW) [33]. The fusion cross section formulas for the Siwek-Wilczynski model (SW) and for the single-Gaussian model are the same, (see Eq. 11 and Ref. [23, 26]), and parameters in the SW model are R_B, V_B and W_B, respectively). In the MSW model, they assumed an energy dependent radius parameter R_B:

$$R_B(Z) = R_0 + \Delta R exp(-Z) erfc(Z). \qquad (15)$$

Here, $Z = \frac{E-V_B}{\sqrt{2}W_B}$, is the same expression used in the single-Gaussian model. The model, with four parameters, does in many cases improve the reproduction property for the cross sections. In some cases, $\Delta R = 0$. And the results are the same as from the SG model.

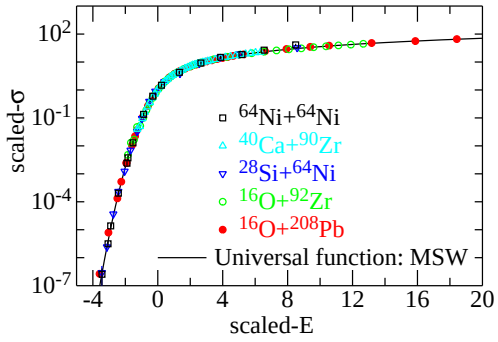


FIG. 4: Spectra of scaled fusion cross sections based on the MSW Model, for the fusion systems ^{16}O + ^{208}Pb [15], ^{16}O + ^{92}Zr [16], ^{28}Si + ^{64}Ni [17], ^{40}Ca + ^{90}Zr [18] and ^{64}Ni + ^{64}Ni [13]. To be compared with Fig. 3(a).

For the MSW model, if one uses:

$$E_B^{scal} = (E - V_B)/(\sqrt{2}W_B), \qquad (16)$$

and

$$\sigma_B^{scal} = \frac{\sigma\sqrt{2}E}{\sqrt{\pi}R_B^2 W_B}, \qquad (17)$$

where, R_B is energy dependent (Eq. 15), then all the data points will be located also very well on the universal function $Y_B(X)$ (Eq. 18), with the $scaled - \sigma$ (Eq. 17) and $scaled - E$ (Eq. 16) on Y-axis and X-axis, respectively:

$$Y_B = \sqrt{\pi}X erfc(-X) + exp(-X^2). \qquad (18)$$

It should be emphasized that, Eq. 18 is exactly the same as Eq. 14, and also Eq. 16 is the same as Eq. 12. Only Eq. 17 is more complex than Eq. 13.

Fig. 4 is the same as Fig. 3, but with the MSW model instead of the single-Gaussian model. That is, Fig. 4 is obtained from Eqs. (16), (17) and (18). The curves in the two figures, Fig. 4 and Fig. 3(a), are the same, and the experimental fusion data are from the same five systems. Although each corresponding point (symbol) is not located at the same place on the two curves, all of them locate well on the two curves, respectively. Evidently, in these two figures, the divergence patterns of all data points from the curves, respectively, are a little different, but can be recognized as at the same level.

The single-Gaussian model is simpler: its expression of σ_{scal} is straight forward in physics, and the reproduction to cross sections is already rather good. The MSW model has one more parameter. The adding of a factor $\Delta R exp(-Z) erfc(Z)$ makes the fitting process more complex, but gains better reproduction to cross sections for many systems. Since there are advantages and disadvantages in each of these two models, and they do supply the same universal function suggested in this article, we recommend both of them to the community.

TABLE II: Results of the least-squares fits of the single-Gaussian barrier distribution model for fusion systems discussed in Fig. 3(b). Parameters are R_g, V_g and W_g, respectively. CN is the compound nucleus, N the number of data points, and 'data-range' is the cross section range of the measured values.

system	CN	N	data-range	R_w	V_w	W_w	Ref.
			mb	fm	MeV	MeV	
^{16}O+^{18}O	^{34}S	21	0.0064-224	7.95	9.89	0.873	[27]
^{16}O+^{154}Sm	^{170}Yb	37	.18-933	10.46	59.27	2.719	[31]
^{11}B+^{197}Au	^{208}Po	17	.00025-770	10.56	46.81	1.780	[28]
^{58}Ni+^{64}Ni	^{118}Ba	11	.0013-166	7.33	94.52	2.144	[32]
^{64}Ni+^{124}Sn	^{188}Pt	12	.0008-126	6.60	152.92	2.303	[29, 30]

Finally, short discussions for the new prescription are given:

1) From the previous section we conclude that a *universal fusion function* can be successfully established from either the single-Gaussian model or the MSW model. It is based on the fact that each of their analytic expressions can reproduce rather well most heavy-ion fusion excitation functions over the wide energy range. In the future, one may find another prescription to give better universal functions, as long as one gets a new fusion cross section formula which reproduces all the experimental fusion data even better, and can get simple, monotonic transformations for the cross section σ and energy E to become the $scaled-\sigma$ and $scaled-E$.

It is known that the multi-Gaussian model (see Ref. [26]) can reproduce fusion cross sections much better than the single-Gaussian model, but one cannot design simple transformations to obtain monotonic $scaled-\sigma$ and $scaled-E$ from this model; thus the multi-Gaussian model cannot be used for this purpose.

2) A universal function of heavy-ion fusion excitation function is beneficial for application, not for a perfect reproduction. The Y-axis of Fig. 3 is logarithmic, spanning about 10 order of magnitudes. The close overlap of the data with the universal function is only approximate. The universal function describes only an average behavior of abundant fusion data.

For various heavy-ion fusion systems, the excitation functions display a small, but nevertheless well established fine structure on top of the average behavior, described by the universal function. These structures are already displayed implicitly in the spectra of barrier distribution at energies higher than the Coulomb barriers e.g. Ref. [4], and have been pointed out explicitly in recent paper, e.g. Ref. [34]. The 'approximation' of the universal function depends on the level of the requirements of an application. It may become more rigid in the future. The level of quantitative approximation of the present approach may be self-evident by the minor deviations appearing in Fig. 3 and in Fig. 4.

3) The Single-Gaussian Model and the MSW model, and the present recipe of obtaining fusion universal function are developed based on the barrier distribution theory, introduced by Rowley *et al.,* [35], a nuclear reaction theory based on a description of entrance-channel effects alone. It seems rather surprising, that the models and the recipe with only entrance-channel parameters and scaling, respectively, describe rather well all individual fusion excitation functions producing compound nuclei over a wide beam energy and mass range, as illustrated in Fig. 3 and Fig. 4.

An interesting question is: by using the single-Gaussian model or MSW model, and applying the transformations, $scaled-\sigma$ and $scaled-E$, the experimental data sit well on a universal fusion function, which does not depend on either the two nuclei in the entrance channel or the compound nucleus. The transformation washes out some properties of the original quantities $\sigma(E)$. Then, what is the remaining effect in the universal function, $Y=\sqrt{\pi}Xerfc(-X)+exp(-X^2)$ itself? It is not a constant value but a monotonic curve. What is the physics meaning of this general behavior of the fusion excitation function? This is an open question. A related question: why does the single-Gaussian model or MSW model reproduce unexpectedly well all the heavy-ion fusion excitation function over a wide energy range? This is not fully understood yet.

The single-Gaussian model was published in 2018 [23]. During the submission of a recent paper, Ref. [36], which used the single-Gaussian model for theoretical calculations, the referee suggested: "As a matter of fact a good reduction method is implicitly given in this manuscript", and listed the transformations (scaling) and the universal function, which are applied in this article. A special acknowledgment is expressed by the authors of the present paper to the referee. The authors also want to thank K. Hagino, A. Stefanini and G. Montagnoli for many valuable discussions.

This work was supported by the US Department of Energy, Office of Nuclear Physics, under Contract No. DE-AC02-06CH11357.

* cjiang@anl.gov

[1] V.I. Zagrebaev, A.S. Denikin, A.V. Karpov, A.P. Alekseev, M.A. Naumenko, V.A. Rachkov, and V.V. Samarin, http://nrv.jinr.ru/.
[2] A.B. Balantekin and N. Takigawa, Rev. Mod. Phys. **70**, 77 (1998).
[3] K. Hagino and N. Takigawa, Prog. Theo. Phys. **128**, 1061 (2012).
[4] M. Dasgupta, D. Hinde, N. Rowley, and A.M. Stefanini, Annu. Rev. Nucl. Part. Sci. **48**, 401 (1998).
[5] B.B. Back, H. Esbensen, C.L. Jiang, and K.E. Rehm, Rev. Mod. Phys. **86**, 317 (2014).

[6] G. Montagnoli and A.M. Stefanini, Eur. Phys. J. A **54**, 218 (2018).

[7] C.L. Jiang, B.B. Back, K.E. Rehm, G. Montagnoli, and A.M. Stefanini, Eur. Phys. J **A 57**, 235 (2021).

[8] P.R.S. Gomes, J. Lubian, I. Padron, and R.M. Anjos, Phys. Rev. **C 71**, 017601 (2005).

[9] L.F. Canto, D.R. Mendes Junoir, P.R.S, Gomes and J. Lubian, Phys. Rev. **C 92**, 014626 (2015).

[10] G.G. Adamian, N.V. Antonenko, H. Lenske, and V.V. Sargsyab, Phys. Rev. **C 109**, 014602 (2024).

[11] C.L. Jiang et al., Phys. Rev. Lett. **89**, 052701 (2002).

[12] C.L. Jiang, H. Esbensen, B.B. Back, R.V.F. Janssens, and K.E. Rehm, Phys. Rev. **C 69**, 014604 (2004).

[13] C.L. Jiang, K.E. Rehm, H. Esbensen, R. V. F. Janssens. B. B. Back, C. N. Davud, J. P. Greene, D. J. Henderson, C. J. Lister, R. C. Pardo, T. Pennington, D. Seweryniak, B. Shumard, S. Sinha, X. D. Tang, I. Tanihata, and S. Zhu, Phys. Rev. Lett. **93**, 012701 (2004).

[14] C.Y. Wong, Phys. Rev. Lett. **31**, 766 (1974).

[15] M. Dasgupta, D.J. Hinde, A. Diaz-Torres, B. Bouriquet, Catherine I. Low, G.J, Milburn, and J.O. Newton, Phys. Rev. Lett. **99**, 192701 (2007).

[16] J.O. Newton, C.R. Morton, M. Dasgupta, J.R. Leigh, J.C. Mein, D.J. Hinde, H. Timmers, and K. Hagino, Phys. Rev. **C 64**, 064608 (2001).

[17] C.L. Jiang *et al.,* Phys. Lett. **B 640**, 18 (2006).

[18] H. Timmers, L. Corradi, A. M. Stefanini, D. Ackermann, J. H. He, S. Beghini, G. Montagnoli, F. Scarlassara, G.F. Segato, and N. Rowley, Phys. Lett. **B 399**, 35 (1997).

[19] C.L. Jiang, Eur. Phys. J **A 58**, 72 (2022).

[20] V.Yu. Denisov and I.Y. Sedykh, Eur. Phys. J. **A. 55,** 153 (2019).

[21] N. Rowley and K. Hagino, Phys. Rev. **C 91**, 044617 (2015).

[22] V.V. Sargsyam, G.G. Adamian, N.V. Antonenko, and W. Scheid, Eur. Phys. J **A 45**, 125 (2010).

[23] C.L. Jiang, K.E. Rehm, B.B. Back, A.M. Stefanini, and G. Montagnoli, Eur. Phys. J **A 54**, 218 (2018).

[24] K. Siwek-Wilczynska, E. Siemaszko, and J. Wilczynski, Acta Phys. Pol. **B 33**, 451 (2002).

[25] K. Siwek-Wilczynska and J. Wilczynski, Phys. Rev. **C 69**, 024611 (2004).

[26] C.L. Jiang and B.P. Kay, Phys. Rev. **C 105**, 064601 (2022).

[27] J. Thomas, Y.T. Chen, S. Hinds, D. Meredith, and M. Olson, Phys. Rev. **C 33**, 1679 (1986).

[28] A. Shrivastava *et al.,* Phys. Rev. **C 96**, 034620 (2017).

[29] C.L. Jiang *et al.,* Phys. Rev. **C 91,** 044602 (2015). (1993); **C 52**, 3151 (1995).

[30] K.T. Lesko, W. Henning, K.E. Rehm, G. Rosner, J.P. Schiffer, G.S.F. Stephans, B. Zeidman, and W.S. Freeman, Phys. Rev. **C 34,** 2155 (1986).

[31] J.R. Leigh, *et al.,* Phys. Rev. **C 47**, R437 (1993); Phys. Rev. **C 52**, 3151 (1995).

[32] A.M. Stefanini *et al.,* Phys. Rev. **C 100**, 044619 (2019).

[33] Y. Chen, H. Yao, M. Liu, J. Tian, P. Wen, and Ning Wang, At. Data and Nucl. Data Tables **154**, 101587 (2023).

[34] C.L. Jiang, W.F. Henning, B.P. Kay, and N. Watwood, Phys. Rev. **C 108,** L051604 (2023).

[35] N. Rowley, G.R. Satchler, and P.H. Stelson, Phys. Rev. Lett. **B 254,** 25 (1991).

[36] C.L. Jiang, W.F. Henning, C.R. Hoffman, B.P. Kay, and N. Watwood, Phys. Rev. **C 108**, L051605 (2023).